Journal of Applied Polymer Science

A pre-polyaddition mediation of castor oil for polyurethane formation

Chandan Sharma,[1] Saji S. Edatholath,[1] A. Raman Unni,[2] T. Umasankar Patro,[3] Vinod K. Aswal,[4] Sangram K. Rath,[5] G. Harikrishnan[1]

[1]Department of Chemical Engineering, Indian Institute of Technology Kharagpur, Kharagpur, West Bengal 721302, India
[2]Automotive and Flexible Foam Division, Huntsman Polyurethanes, Navi Mumbai, Maharashtra 400710, India
[3]Department of Materials Engineering, Defence Institute of Advanced Technology, Pune, Maharashtra 411025, India
[4]Solid State Physics Division, Bhabha Atomic Research Centre, Mumbai, Maharashtra 400085, India
[5]Polymer Division, Naval Materials Research Laboratory, Ambernath, Maharashtra 421506, India
Correspondence to: G. Harikrishnan (E-mail: hari@iitkgp.ac.in)

ABSTRACT: We report a simple, serendipitous, two step mediation that overcomes the polyaddition threshold of castor oil during polyurethane formation. The mediation facilitates formation of polyurethane systems directly from castor oil without triricinolein chain extension or the use of supplementary hydroxyl compounds. The mediation involves refluxing castor oil with *n*-Butyl lithium in the presence of a solvent followed by water addition. We demonstrate the effectiveness of this mediation by successfully generating two important polyurethane systems (foam and coating) from castor oil. We identify that the mediation introduces two new compounds in castor oil namely, a lithiated diglyceride and a lithium salt of fatty acid. We characterize the new polyurethane synthesized for their hard-soft segmented morphology, glass transition temperature, and thermomechanical properties. © 2016 Wiley Periodicals, Inc. J. Appl. Polym. Sci. **2016**, *133*, 43964.

KEYWORDS: biopolymers & renewable polymers; coatings; foams; polyurethanes

Received 22 February 2016; accepted 22 May 2016
DOI: 10.1002/app.43964

INTRODUCTION

The versatility of segmented polyurethane arises due to tailorable nature of polyaddition reaction between hydroxyl and isocyanate functionalities. This enables the formation of numerous polyurethane systems such as foams, coatings, adhesives, sealants, and biomedical implants. Castor oil is a major renewable hydroxyl component used in polyurethane synthesis. The inherent presence of hydroxyl functional groups in its triricinolein fraction makes it an attractive plant derived renewable hydroxyl compound for polyurethane synthesis.[1–24] However, triricinolein has limited reactivity with isocyanate functional groups due to several factors such as secondary functionality of hydroxyl groups, and steric effects of the dangling chain.[1–8] These factors manifest in several ways during polyaddition reaction as slow kinetics, insufficient molecular weight buildup, low rate of cross-linking, and high sol-fraction. It is almost impossible to overcome these deficiencies in pure castor oil generated polyurethane systems, even while the reaction is conducted in the presence of significant concentration of urethane catalysts.[24] These deficiencies are generally overcome by employing one or more of the following methods. A common way is to use other highly reactive supplementary compounds along with castor oil. This, however, severely limits the usable volume fraction of castor oil.[7,8,13,17,24] Another way is to chemically modify triricinolein chains so as to enhance the reactivity.[21–24] This method requires complex and extensive chemical modification process.

In this article, we report a simple, serendipitous, two step mediation that substantially enhanced castor oil reactivity with isocyanate moieties and successfully generated polyurethane systems. This process involved refluxing pure castor oil with *n*-Butyl lithium in the presence of a solvent, followed by water addition. The reaction mixture is distilled and the residue is used for polymerization. We demonstrate that having all other ingredients and procedure remaining the same, while pure castor oil does not react, the new mediation successfully generates stable polyurethane foams and free standing films of coating. This indicates a simple pathway to generate various polyurethane systems completely from castor oil without extensive chain modification of triricinolein or using supplementary hydroxyl compounds.

EXPERIMENTAL

Formulation

We used standard formulations of urethane catalysts/surfactants that are employed for polyurethane foam and coating system generation. During both syntheses, we kept the weight fraction of castor oil and mediated castor oil, the same. The mass of

isocyanate was calculated based on approximate molar ratio of [NCO]:[OH] = 0.97:1 (isocyanate index = 97) for polyurethane foams and 1:1 (isocyanate index = 100) for coating. These estimations were for hydroxyl functionality of pure castor oil. The pre-polyaddition mediation was conducted as follows. 50 mL of castor oil (Loba Chemie) having a hydroxyl value of 163 and molecular weight of 930 was dissolved in 500 mL of tetrahydrofuran (HPLC Grade, Sigma-Aldrich), using a magnetic stirrer. This mixture was kept in an ice bath to which *n*-butyllithium (1.6 *M* in hexane, Rockwood lithium) was added drop wise. The molar ratio of *n*-butyl lithium to castor oil was 3.2:1. The mixture was again stirred for 40 min. Distilled water was slowly added (at a molar ratio of 1:1 to that of *n*-BuLi) to the mixture and was stirred again for 30 min. The whole mixture was then distilled using a batch distillation set-up at a temperature of 65 °C. The residue of the distillation unit was collected and its volume was reduced to the initial volume of pure castor oil by evaporation conducted at 70 °C, in a round bottom flask. This mixture is hereafter designated in the article as mediated/modified castor oil (MCO) while as pure castor oil is referred as CO.

Polyurethane Synthesis Procedure

For generation of polyurethane foams, the isocyanate component used was a polymeric 4, 4′ diphenyl methane diisocyanate (Suprasec 6456, Huntsman Polyurethanes). Foaming agents used were surfactant (Tegostab 8734 LF, Evonik), catalysts bis(2-dimethylaminoethyl)ether (Niax A-1, Momentive), diethanolamine (Sigma-Aldrich) and a mixture of triethylenediamine and dipropyleneglycol (Dabco 33-LV, Sigma Aldrich), and distilled water. CO/MCO (93.3 parts by weight (pbw) was blended with distilled water (4.2 pbw), catalyst blend (Niax A-1 = 0.1 pbw, diethanolamine = 0.3 pbw, Dabco 33-LV = 0.35 pbw), and surfactant (0.5 pbw) into a paper cup of volume 600 mL. The blend was stirred at an approximate speed of 3000 rpm using a mechanical stirrer (RQ-122, Remi). The isocyanate component was added to the blend of hydroxyl component, catalyst and surfactant at a weight ratio of 65:100 and stirred at a speed of 4000 rpm for 15 s. The foam was allowed to expand freely. After expansion, the foam was kept for curing in vacuum oven at 80 °C for 48 h. For coating, the isocyanate component used was an aliphatic isophorone diisocyanate (IPDI, Fluka). 20 g of CO/MCO was taken and refluxed with 20 mL of toluene (Sigma-Aldrich) at 70 °C, using a coupled magnetic stirrer cum heater (Tarson Digital Spinot). While CO quickly dissolved in toluene, MCO initially appeared as small lumps, but dissolved on continued refluxing. This solution was transferred into a conical flask and heated to 100 °C and two drops of catalyst [dibutyltin dilaurate (DBTDL), Sigma-Aldrich] was added. 25 mL of IPDI which is taken in a syringe is added drop by drop to this mixture, while the temperature was maintained at 100 °C. The slow, drop wise addition of IPDI took about 1 h to complete (immediate addition was found to produce large number of bubbles in the case of MCO, creating defects in cured films). After complete addition of IPDI and the elapse of 15 min, the solution viscosity started increasing for mediated castor oil while as no visible change was observed for pure castor oil. At the immediate observation of the first bubble (for MCO), the conical flask was transferred to a vacuum oven, to remove the bubbles. After that, the solution was poured into a petri dish and allowed to cure at ambient conditions. The reaction mixture of pure castor oil did not show any visible change with time and remained in the uncured liquid state, even after several days.

CHARACTERIZATIONS

We characterized castor oil before and after mediation by the following techniques. Fourier transform infrared spectroscopy (Spectrum 100, Perkin Elmer) was used to analyze functional groups. The scan speed was 0.2 cm/s and the resolution was 4 cm^{-1}. The fractional composition was analyzed by HPLC (Perkin Elmer, Series 200 UV-Vis detector). About 20 μL sample was injected into an Agilent Zorbax SB C-18 reverse phase HPLC column with a UV detector (wavelength 205 nm, Perkin Elmer Series 200). The mobile phase was a mixture of ethanol and water, at a volume ratio 90:10. The flow rate was 1 mL/min. The molecular weights of components were investigated by MALDI-TOF spectroscopy (MALDI ToF/ToF Ultraflexar, Bruker). Matrix solution was prepared using a mixture of acetonitrile and triflouroacetic acid solution, in which a pinch of α-cyano-4-hydroxycinnamic acid and 2,5-dihydroxy benzoic acid were present. Analyte solution was prepared by dissolving 10 mg of CO/MCO in methanol. A MALDI-ToF test solution was prepared by mixing matrix solution and analyte solution in equal proportion. About 1 μL of test solution was placed in the well of the sample plate and the solvent was allowed to evaporate. Sample plate was placed under MALDI ion source. Positive ion MALDI spectra (1500 scans) were acquired in reflection mode using Smartbeam–II laser (accelerating voltage = 20.3 kV). NMR spectroscopy was conducted using an Avance III 500 NMR spectrometer (Bruker) using $CDCl_3$ as solvent. 5 mg of sample was dissolved in 1 mL of solvent in a small vial and transferred to 5 mm NMR tubes using a glass pipette.

Polyurethanes systems were characterized by following techniques. For sol-fraction estimation, foam/coating samples were kept in dimethyl formamide for 3 days. These samples were then transferred into a vacuum oven and kept there at 80 °C, till the weight of samples remained unchanged. Percentage difference between initial and final weight gave sol fraction. FTIR was used to identify urethane and carbonyl functional groups. Scan speed was 0.2 cm/s and the resolution was 4 cm^{-1}. Polymer morphology was visualized by high resolution transmission electron microscopy (JEOL, JEM-2100). Samples for HRTEM were prepared using cryo-microtome (Phillips CM-12) at −100 °C. Microtomed samples of approximate thickness 60 nm were mounted on copper grids, using sucrose solution. Small angle neutron scattering conducted at the National facility for neutron beam research (Bhabha Atomic Research Centre, Mumbai) was additionally used to investigate polymer morphology in foams. The mean incident radiation wavelength was 5.2 Å with $\Delta\lambda/\lambda = 15\%$. Scattering data were taken on an absolute scale using standard protocols and were corrected for the background, transmission, and the empty cell contributions. Since coating synthesized did not give sufficient contrast to neutrons, we used small angle X-ray scattering. The measurements were carried out using a SAXS system (SAXSess MC^2, Anton Paar)

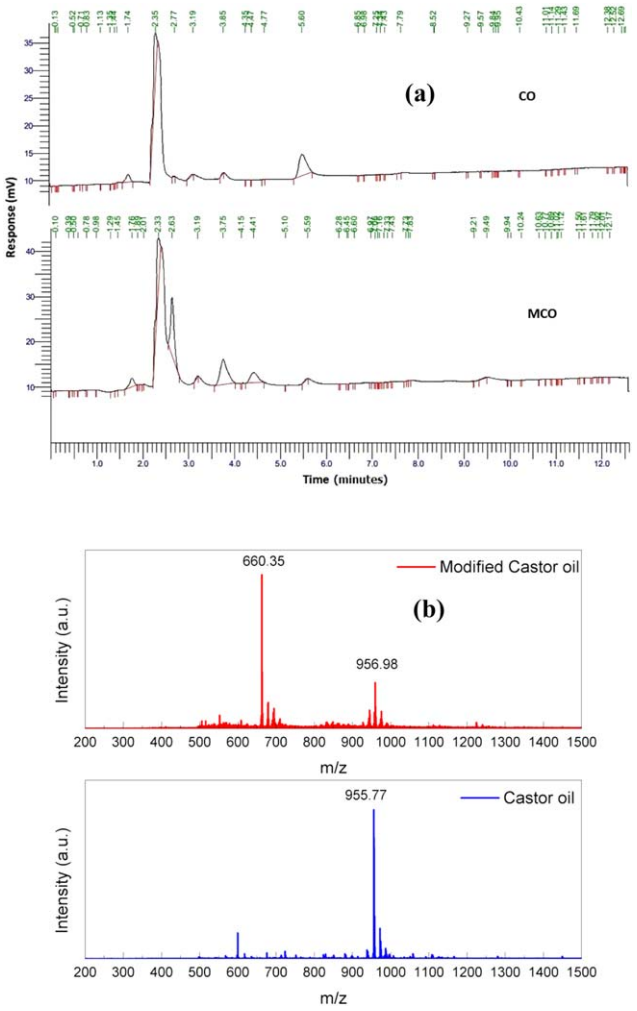

Figure 1. (a) HPL Chromatogram; (b) MALDI-TOF of CO and MCO. [Color figure can be viewed in the online issue, which is available at wileyonlinelibrary.com.]

operated in line-collimation mode with Cu-K_α X-ray source of $\lambda = 0.154$ nm and a sample-to-detector distance of 309 mm. The samples were scanned for 10 min (exposure time: 10 s, no. of frames: 60) followed by subtraction of dark current and desmearing. Both neutron and X-ray scattering traces were analyzed using a SASfit program (Paul Scherrer Institute, Switzerland). A differential scanning calorimeter (Q20, TA Instruments) was used to estimate the glass transition temperature. Approximately 2 mg of powdered sample was loaded into an aluminum pan and sealed hermetically before experiments. Samples were cooled from room temperature to −60 °C at a ramp of 3 °C/min. The thermal stability was analyzed using a thermogravimetric analyzer (Q50, TA instruments). Approximately 10 mg mass of samples of crushed polyurethane were loaded in a platinum crucible. The experiment was performed under N_2 atmosphere from 24 to 500 °C at heating rate of 10 °C/min. Mechanical properties were estimated by a universal testing machine (Tinius Olsen H50KS). Foams of dimensions 80 × 20 × 5 mm and films of dimensions 100 × 15 × 1 were used. The stretch rate for foams was 10 mm/min. The stretch rate for films was 2 mm/min. A software (Test Navigator) analyzed the stress–strain relationship and estimated tensile strength at break and percentage elongation.

RESULTS AND DISCUSSION

Mediated Castor Oil

We analyze the composition of pure and mediated castor oil by a combination of HPL chromatography as well as MALDI-ToF, FTIR, and NMR spectroscopic techniques. Based on these analyses, we also propose a reaction scheme for conversion of CO to MCO. In the HPL chromatogram shown in Figure 1(a), a major peak at a retention time of 2.4 min is seen repeating for both CO and MCO. This peak represents the parent triricinolein. Smaller peaks representing minor fractions of other fatty acids are also seen in both cases. For MCO, the presence of two additional compounds is evident by the occurrence of two new significant peaks at 2.63 min (one with relatively higher intensity appearing as a split peak to the main triricinolein peak) and another one at 4.42 min. Figure 2 (top figure) shows the FTIR spectra for both CO and MCO. Compared to spectra of pure castor oil, two additional peaks (at 1577 cm^{-1} and 1548 cm^{-1}) are present in MCO. These peaks confirm presence of RCOO-

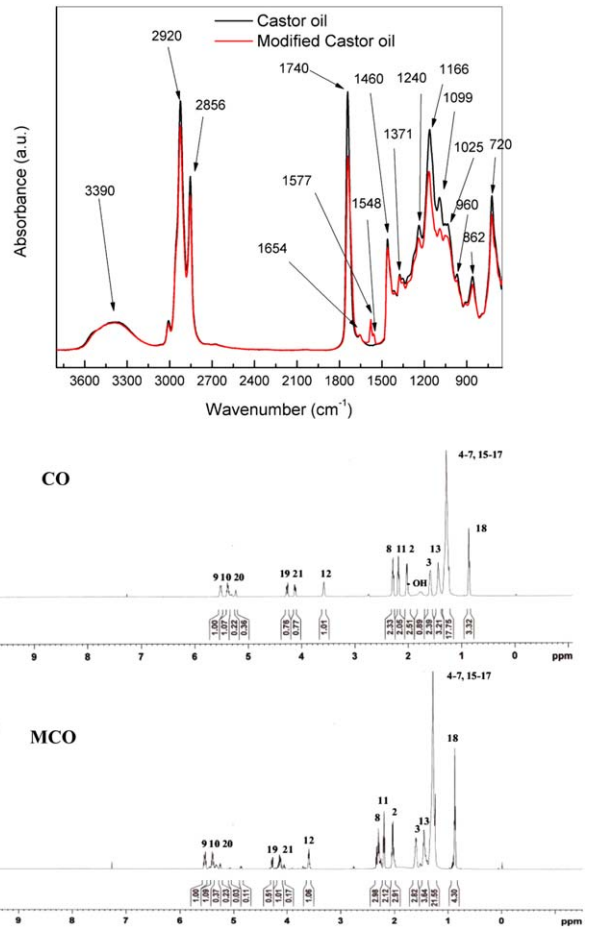

Figure 2. FTIR (top) and H NMR (bottom) spectra of CO and MCO. [Color figure can be viewed in the online issue, which is available at wileyonlinelibrary.com.]

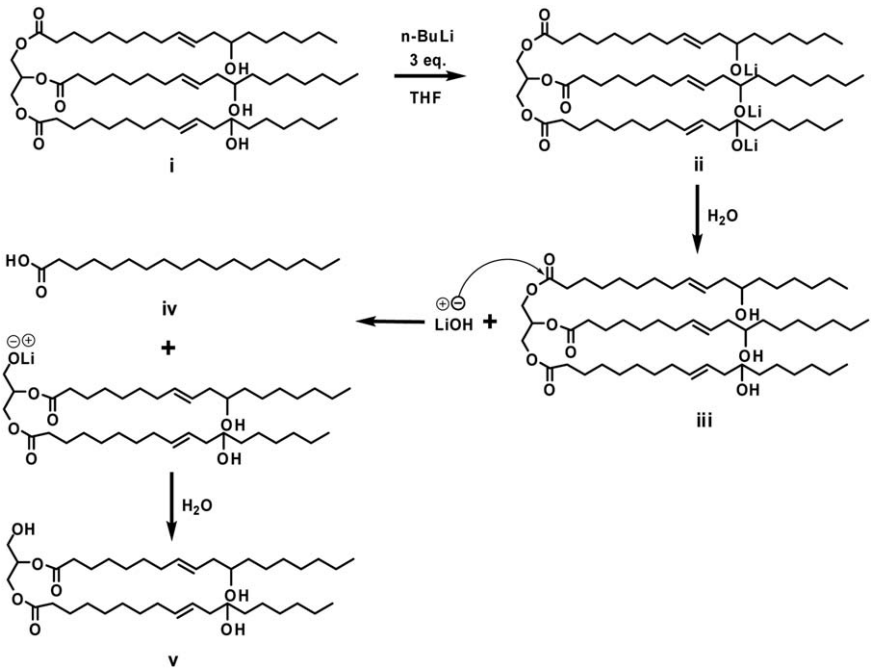

Figure 3. A plausible mechanism, showing the conversion of ricinoleic acid to a lithiated diglyceride and a lithium salt of fatty acid. This mechanism is based on the evidences obtained from HPL chromatography as well as FTIR, MALDI-ToF, and NMR spectroscopies.

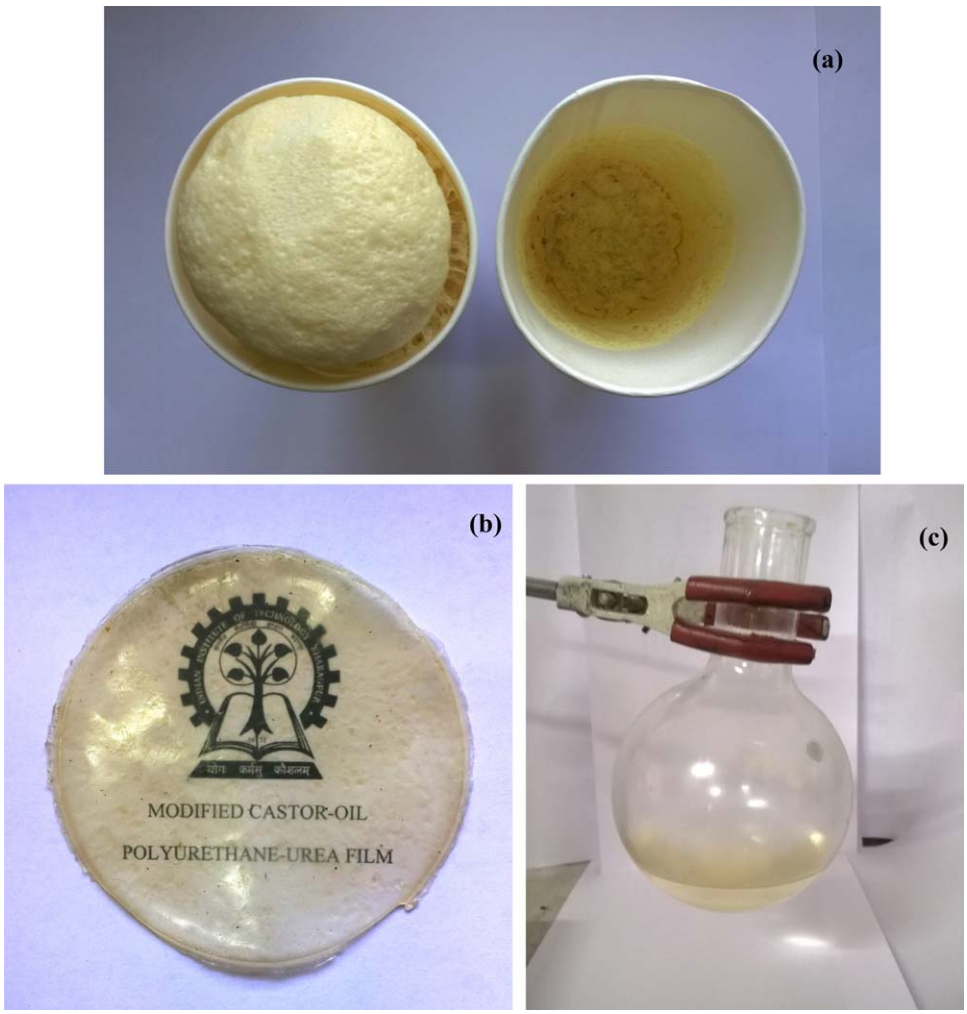

Figure 4. (a) Polyurethane foams generated with (left) and without (right) mediation; (b) polyurethane coating generated with mediation; (c) unreacted mixture of castor oil and IPDI in the absence of mediation. [Color figure can be viewed in the online issue, which is available at wileyonlinelibrary.com.]

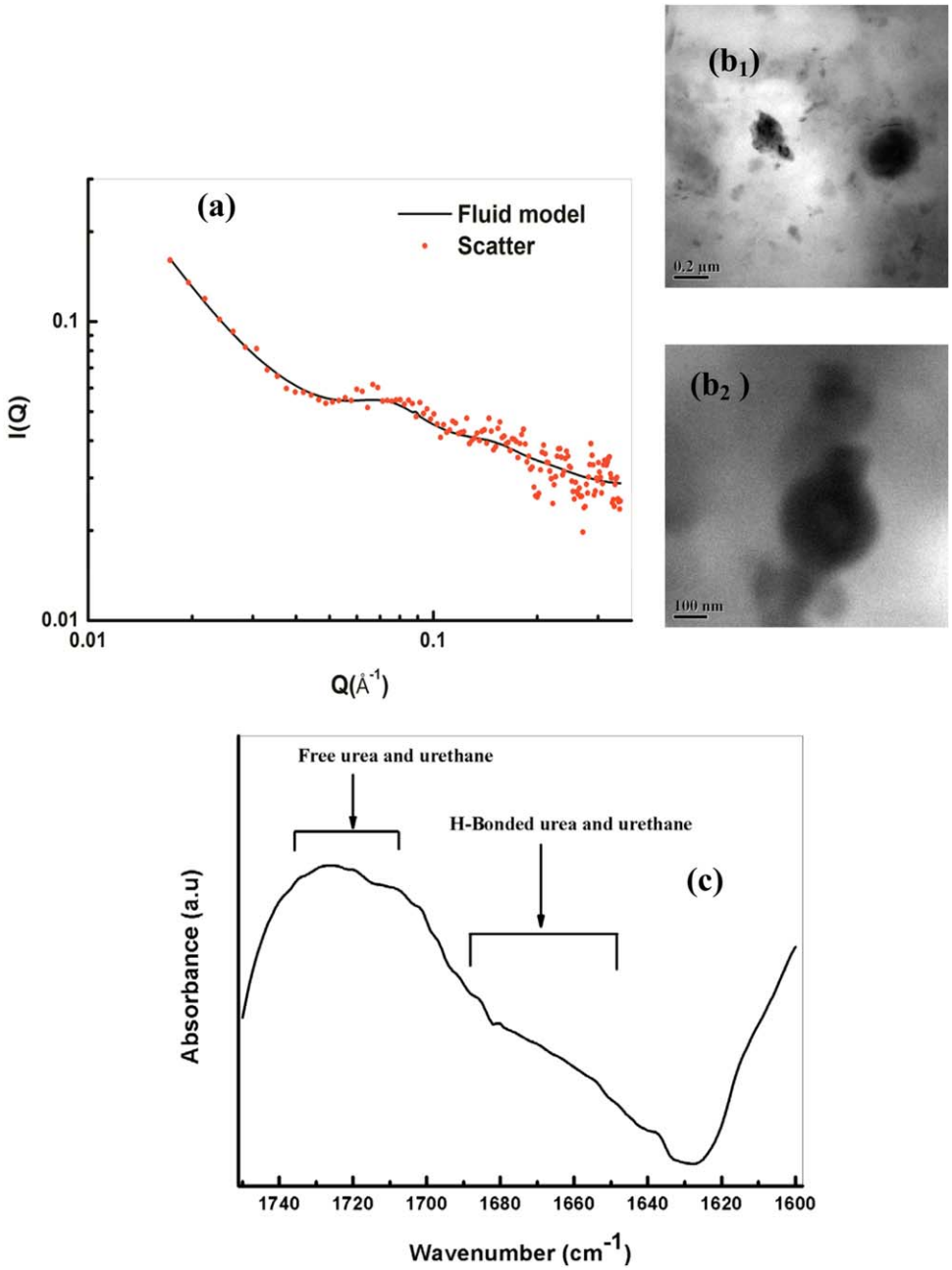

Figure 5. Polyurethane foam: (a) small angle neutron scattering traces; (b_1,b_2) transmission electron microscope images; and (c) FTIR spectra. [Color figure can be viewed in the online issue, which is available at wileyonlinelibrary.com.]

Li+ complex. Figure 1(b) shows the MALDI-TOF spectra of CO and MCO. Spectra for castor oil show an m/z peak at 955.77 as the dominating signal. This corresponds to the molecular weight of triricinolein.[25,26] A similar peak is seen in MCO spectra at a molecular weight of 956.98. In addition, the spectra of MCO also show a dominant m/z signal at a molecular weight of 660.35. Based on this molecular weight, we interpret this compound as a lithiated diglyceride species, which is identified by HPLC at the retention time of 2.63 min. The presence of $COOLi^+$ group shown in FTIR is interpreted to be due to lithium salt of 12-hydroxy stearic acid. This is also confirmed by presence of the peak at the retention time 4.42 min in MCO by HPLC. Figure 2(b) shows the ^{1}HNMR spectrum of CO and MCO. In the spectra of CO, the fatty acid protons [(—CH_2)CO—] are identified in the range of $\delta = 2.2–2.4$ ppm (peak numbered as 2) the methyl protons are identified at $\delta = 0.85$ ppm (peak no. 18) and the glyceride protons between $\delta = 4.1$ and 4.3 ppm (peak nos. 19 & 21). Methylene proton attached to hydroxyl group is seen at 3.58 ppm (peak 12). Proton related to —OH group appeared at 1.5 ppm (indicated by

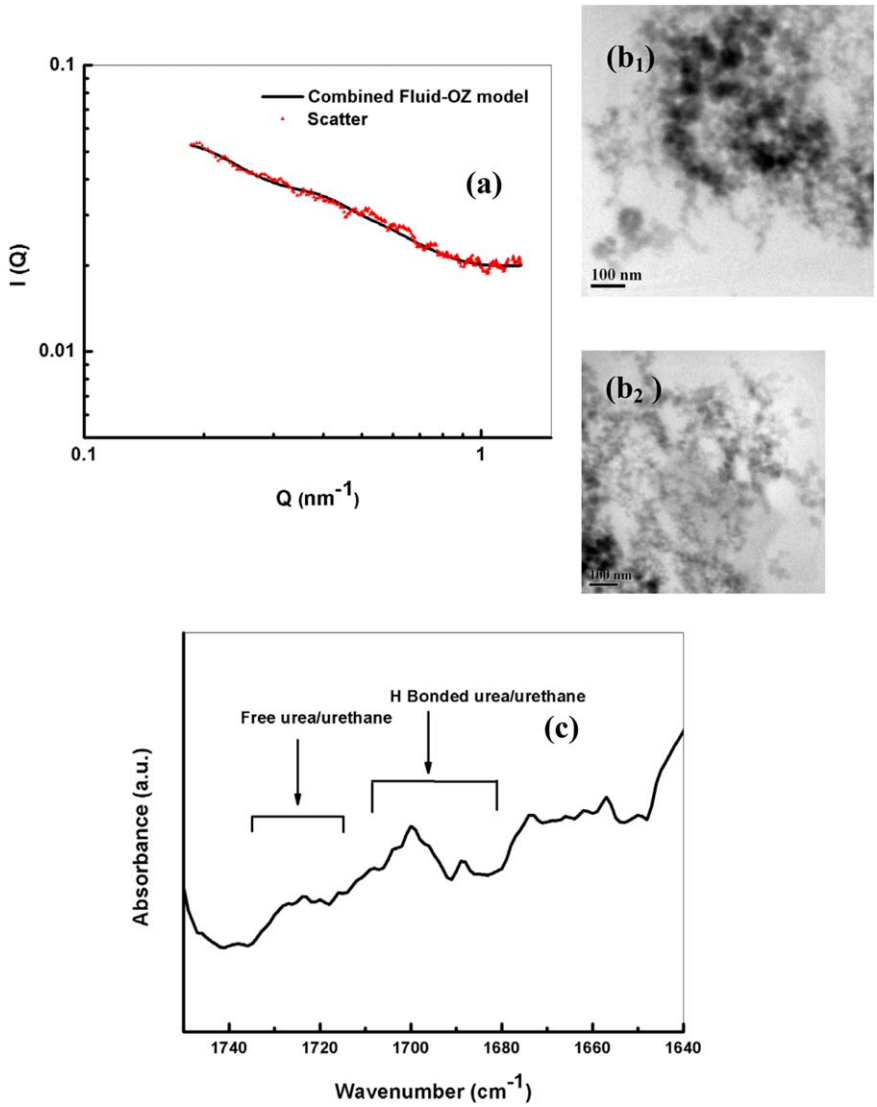

Figure 6. Polyurethane coating: (a) small angle X-ray scattering traces; (b_1,b_2) transmission electron microscope images; and (c) FTIR spectra. [Color figure can be viewed in the online issue, which is available at wileyonlinelibrary.com.]

OH in the spectra). In the case of MCO, although the peak intensity varies for the same protons, the peak positions do not change.

The proposed mechanism is shown in Figure 3. Since castor oil has about 90% ricinoleic acid content, 1 mole of castor oil has roughly 2.7 mole of —OH groups. When *n*-Butyl lithium is added to castor oil, it will most likely induce deprotonation and form Butane and lithium alkoxylate of ricinoleic acid. Note that, a molar ratio of 3.2 between *n*-BuLi and castor oil was used in the reaction. Hence, 2.7 moles of *n*-BuLi will react with hydroxyl groups of ricinoleic acid and form lithium alkoxylate. On adding water and refluxing, this mixture can undergo hydrolysis forming lithium salts of ricinoleic acid and diglyceride along with the possibility of formation of very small amounts of monoglycerides and glycerol.

New Polyurethane Systems

Figures 4 show digital images of polyurethane foams and coating systems generated from CO and MCO. While no discernible foams could be made from CO, those synthesized from MCO are clearly stable. Similarly, while coating made from MCO can be collected as free standing films in about one day, those made from CO remained in the uncured liquid state [Figure 4(c)]. Sol-fraction for foams and coating synthesized from MCO was found to be nominal at (3.9 ± 0.2) % and (8.5 ± 0.5) %, respectively. This indicates high urethane conversion and cross-linking. Two major reasons could be attributed for overcoming the threshold for polyaddition and high conversion and cross linking with MCO. The —OLi group of the diglyceride in MCO can undergo hydrolysis and can give a compound with a primary hydroxyl group (compound v in Figure 3). Primary hydroxyl groups can

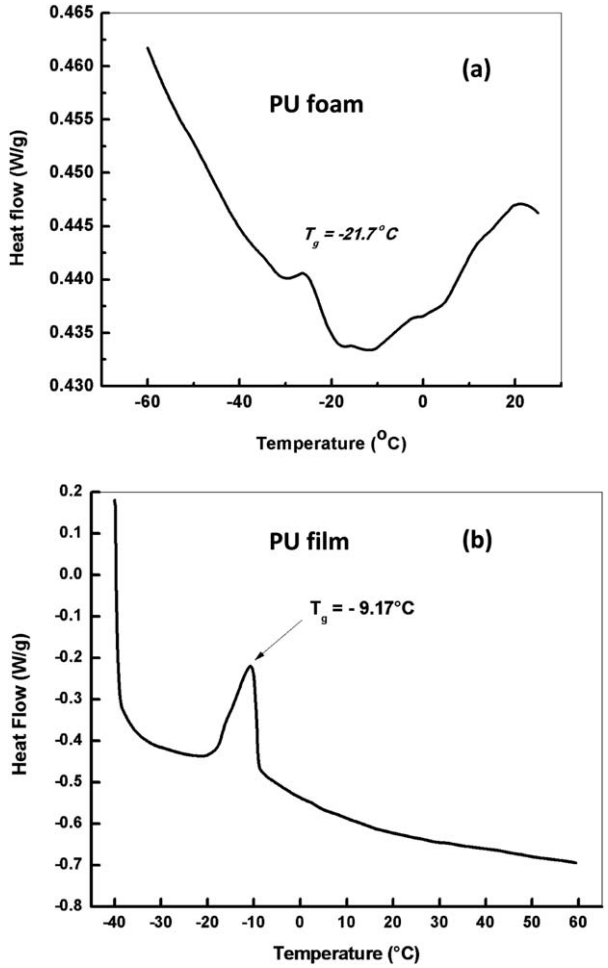

Figure 7. Differential scanning thermograms and estimated glass transition temperatures of new polyurethane systems.

react faster than the inherent secondary hydroxyl groups of triricinolein. The alkoxides of carboxylic acid (the second compound in iv) can catalyze urethane reaction.[27]

Segmented Polymer Morphology

Now, we conduct analysis of morphology of new polyurethanes and identify that the presence of lithium might have influenced the block segmentation. TEM micrographs [Figure 5(b1,b_2)] show nearly spherical, discrete hard domains in the soft matrix of polymer phase of foams. FTIR spectra in the carbonyl stretching region of foams [Figure 5(c)] shows that, while the concentration of free urethane and urea domains (peaks appearing between 1730 and 1710 cm^{-1} with prominent peaks at 1730 and 1720 cm^{-1}) is significant, that corresponding to hydrogen bonded domains (peaks of very low intensity occurring between 1680 and 1650 cm^{-1}) are negligible. This corroborates the existence of a morphology, with well separated individual hard domains. Based on TEM and FTIR observation, we select a fluid model to extract quantitative information of hard domains from SANS traces [Figure 5(a)] of foams. This model envisages discretely dispersed hard sphere morphology in a continuous soft matrix.[28] We estimate the long range periodicity between hard domains as 18.7 nm, the volume fraction of hard domains as 0.157 and average domain size as 30 nm. For coating, the morphology shows a different pattern of domain segmentation. TEM micrographs [Figure 6(b1,b_2)] show the presence of mostly connected hard domains, although a few individual smaller domains that are well separated are also observed. The lower intensity of peaks corresponding to free domains compared to hydrogen bonded domains seen in FTIR spectra [Figure 6(c)] corroborates this state of dispersion. Inspired by this observation, we use a combined fluid and Ornstein-Zernik model to extract quantitative information from SAXS traces [Figure 6(a)] of films. This combined model accounts for the presence of both discrete and continuum structures.[29] We estimate the radius of individual domains to be 8.2 nm, the correlation length of connected domain clusters to be 917.6 nm and the volume fraction to be 0.16. In the presence of lithium compounds, the hard domain segmentation is well known to be affected. This is due to the influence of lithium ions on hydrogen bonding between hard domains.[30] Since the diglyceride and fatty acid are present as lithium salts, the solvation of lithium ions during polyurethane formation is expected to influence hydrogen bonding, which is also evident from the difference between intensity of hydrogen bonded and free hard domains as seen in FTIR spectra [Figures 5(c) and 6(c)]. The polar lithiated carboxylic group of the new compound can phase separate and form individual phase.[31]

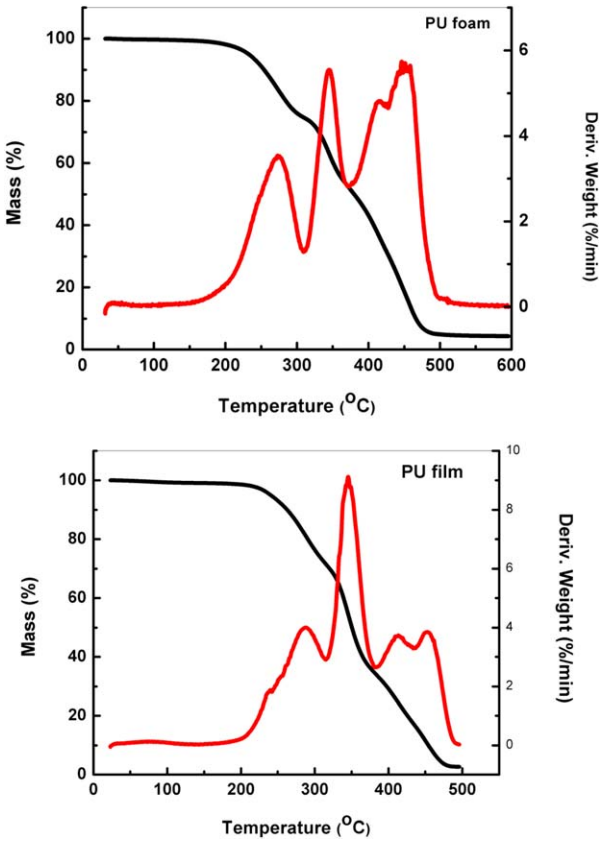

Figure 8. Thermal degradation profiles of new polyurethane systems. [Color figure can be viewed in the online issue, which is available at wileyonlinelibrary.com.]

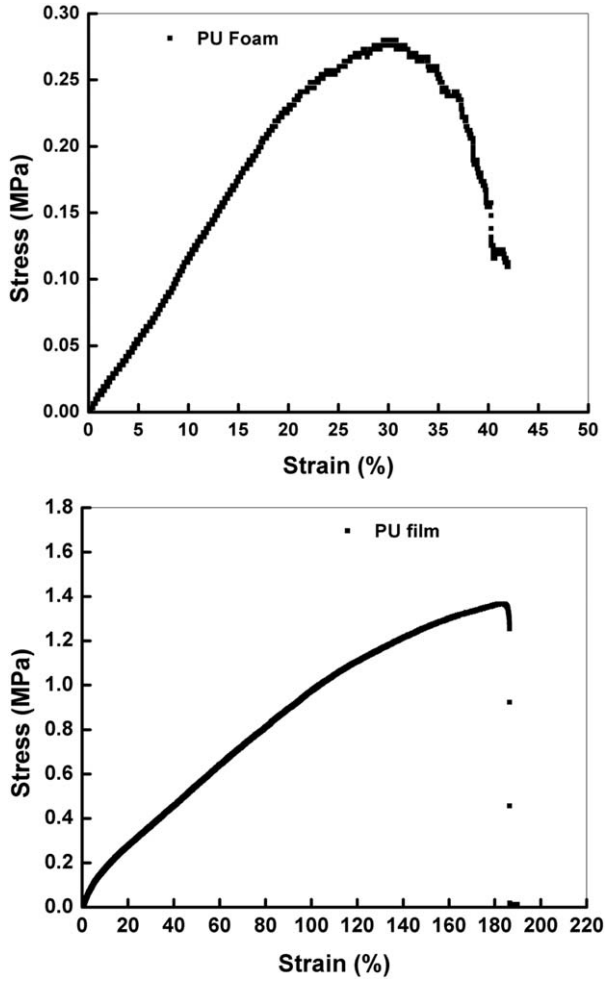

Figure 9. Stress–strain relationship of new polyurethane systems.

Glass Transition Temperature and Thermomechanical Properties

The estimation of thermomechanical properties and glass transition temperature of new polyurethanes follow. The glass transition temperature of the soft domain was found at −21.7 °C for foams and at −9.2 °C for coating (Figure 7). Figure 8 shows the thermogravimetric profile. The thermal decomposition of polyurethane occurs in two steps.[32] The first decomposition starts at approximately 200 °C indicating the onset of decomposition of urethane and urea bond breaking. A later decomposition after 350 °C, where the high temperature peak can be related to the breakdown of polyether groups is also seen. In the first step, approximately 30% and 27% mass losses were recorded between 200 and 320 °C for PU coating and foam, respectively. In the second decomposition step (temperature range between 320 and 480 °C), approximately 70% and 68% mass loss occurred for coating and foams, respectively. The tensile strength at break estimated from the stress–strain profile (Figure 9) was at 0.26 ± 0.05 MPa for foams and 1.37 ± 0.6 MPa for coating. The percentage elongations were recorded at 41.6 ± 2% and 199.5 ± 5% for foams and coating, respectively.

CONCLUSIONS

In summary, we generated polyurethane from castor oil after a two step mediation conducted before polyaddition. This mediation that employed *n*-butyl lithium and water enabled the successful generation of polyurethane foams and coating directly from castor oil without extensive chain modification of ricinoleic acid or resorting to the use of supplementary hydroxyl compounds. We identify the presence of a lithiated diglyceride and a minor fraction of lithium salt of carboxylic acid in mediated castor oil. However, the major fraction remains to be the parent triricinolein. We also characterized the new polyurethanes formed for their segmented morphology, glass transition temperature and thermomechanical properties. Our primary analysis indicated the presence of lithium in the two splinter compounds formed. This lithium can be solvated during polyurethane formation and might have significantly influenced the hard-soft segmented polymer morphology of new polyurethanes systems generated.

ACKNOWLEDGMENTS

G. Harikrishnan acknowledges the financial support from UGC-DAE consortium for scientific research through grant number CRS-M-171. The beam time provided at National facility for neutron research, Bhabha Atomic Research Center, Mumbai is also acknowledged. The authors are grateful to Huntsman Polyurethanes for materials. Parts of this work were carried out at the central research facility of the Indian Institute of Technology Kharagpur.

REFERENCES

1. Engels, H. W.; Pirkl, H. G.; Albers, R.; Albach, R. W.; Krause, J.; Hoffmann, A.; Casselmann, H.; Dormish, J. *Angew. Chem. Int. Ed.* **2013**, *52*, 9422.
2. Ying, X.; Larock, R. C. *Green Chem.* **2010**, *12*, 1893.
3. Pfister, D.; Xia, Y.; Larock, R. C. *ChemSusChem* **2011**, *4*, 703.
4. Lligadas, G.; Ronda, J. C.; Galia, M.; Cadiz, V. *Biomacromolecules* **2007**, *8*, 1858.
5. Petrovic, Z. S. *Polym. Rev.* **2008**, *48*, 109.
6. Desroches, M.; Escouvois, M.; Auvergne, R.; Caillol, S.; Boutevin, B. *Polym. Rev.* **2012**, *52*, 38.
7. Palaskar, D. V.; Boyer, A.; Cloutet, E.; Alfos, C.; Cramail, H. *Biomacromolecules* **2010**, *11*, 1202.
8. Lligadas, G.; Ronda, J. C.; Galia, M.; Cadiz, V. *Biomacromolecules* **2010**, *11*, 2825.
9. Aranguren, M. L.; Rácz, I.; Marcovich, N. E. *J. Appl. Polym. Sci.* **2007**, *105*, 2791.
10. Petrović, Z. S.; Cvetković, I.; Hong, D.; Wan, X.; Zhang, W.; Abraham, T.; Malsam, J. *J. Appl. Polym. Sci.* **2008**, *108*, 1184.
11. Rajalingam, P.; Radhakrishnan, G. *Polym. Int.* **1991**, *25*, 87.
12. Hablot, E.; Zheng, D.; Bouquey, M.; Avérous, L. *Macromol. Mater. Eng.* **2008**, *293*, 922.

13. Rio, E. D.; Lligdas, G.; Ronda, J. C.; Galia, M.; Meier, M. A. R.; Cadiz, V. J. *J. Polym. Sci. Part A: Polym. Chem.* **2011**, *49*, 518.

14. Thakur, S.; Karak, N. *Prog. Org. Coat.* **2013**, *76*, 157.

15. Wang, H. J.; Rong, M. Z.; Zhang, M. Q.; Hu, J.; Chen, H. W.; Czigány, T. *Biomacromolecules* **2008**, *9*, 615.

16. Yeadon, D. A.; McSherry, A. W. F.; Goldblatt, L. A. *J. Am. Oil Chem. Soc.* **1959**, *36*, 16.

17. Tran, N. B.; Pham, Q. T. *Polymer* **1997**, *38*, 3307.

18. Liu, D.; Tian, H.; Zhang, L.; Chang, P. R. *Ind. Eng. Chem. Res.* **2008**, *47*, 9330.

19. Suresh, K. I.; Thachil, E. T. *Angew. Makromol. Chem.* **1994**, *218*, 127.

20. Sharma, C.; Kumar, S.; Unni, A. R.; Aswal, V. K.; Rath, S. K.; Harikrishnan, G. *J. Appl. Polym. Sci.* **2014**, *131*, DOI: 10.1002/app.40668.

21. Zhang, C.; Xia, Y.; Chen, R.; Huh, S.; Johnston, P. A.; Kessler, M. R. *Green Chem.* **2013**, *15*, 1477.

22. Zhang, C.; Madbouly, S. A.; Kessler, M. R. *ACS Appl. Mater. Interfaces* **2015**, *7*, 1226.

23. Zhang, C.; Kessler, M. R. *ACS Sustainable Chem. Eng.* **2015**, *3*, 743.

24. Allauddin, S.; Narayan, R.; Raju, K. V. S. N. *ACS Sustainable Chem. Eng.* **2013**, *1*, 910.

25. Ayorinde, F. O.; Elhilo, E.; Hlongwane, C. *Rapid Commun. Mass Spectrom.* **1999**, *13*, 737.

26. Ayorinde, F. O.; Garvin, K.; Saeed, K. *Rapid Commun. Mass Spectrom.* **2000**, 608.

27. Sardon, H.; Engler, A. C.; Chan, J. M. W.; Garcia, J. M.; Coady, D. J.; Pascual, A.; Jones, D. O. M.; Rice, J. E.; Horn, H. W.; Hedrick, J. L. *J. Am. Chem. Soc.* **2013**, *135*, 16235.

28. Mang, J. T.; Hjelm, R. P.; Orler, E. B.; Wrobleski, D. A. *Macromolecules* **2008**, *41*, 4385.

29. Laity, P. R.; Taylor, J. E.; Wong, S. S.; Khunkamchoo, P.; Norris, K.; Cable, M.; Andrews, G. T.; Johnson, A. T. F.; Cameron, R. E. *Polymer* **2004**, *45*, 7273.

30. Sheth, J. P.; Aneja, A.; Wilkes, G. L. *Polymer* **2004**, *45*, 5979.

31. Zhang, L.; Brostowitz, N. R.; Cavicchi, K. A.; Weiss, R. A. *Macromol. React. Eng.* **2014**, *8*, 81.

32. Delbecq, E.; Pascault, J.-P.; Boutevin, B.; Ganachaud, F. *Chem. Rev.* **2013**, *113*, 80.